Available online at www.sciencedirect.com

ScienceDirect

journal homepage: www.elsevier.com/locate/he

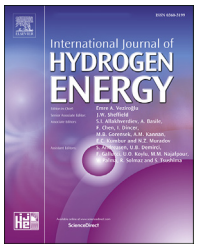

Construction of three-dimensional hierarchical Pt/TiO_2@C nanowires with enhanced methanol oxidation properties

Yanan Guo [a,b], *Limei Tang* [a,b], *Yong Zhang* [a,b,*], *Haoshan Wei* [a,b], *Xia Shu* [a,b], *Jiewu Cui* [a,b], *Yan Wang* [a,b], *Jiaqin Liu* [b,c], *Quanzhong Li* [d], *Xueliang Sun* [e], *Yucheng Wu* [a,b]

[a] *School of Materials Science and Engineering, Hefei University of Technology, Hefei, 230009, PR China*
[b] *Key Laboratory of Advanced Functional Materials and Devices of Anhui Province, Hefei, 230009, PR China*
[c] *Institute of Industry & Equipment Technology, Hefei University of Technology, No.193 Tunxi Road, Hefei, 230009, Anhui, PR China*
[d] *School of Resources and Environmental Engineering, Hefei University of Technology, No.193 Tunxi Road, Hefei, 230009, Anhui, PR China*
[e] *Department of Mechanical and Materials Engineering, The University of Western Ontario, London, N6A 5B9, Ontario, Canada*

HIGHLIGHTS

- 3D TiO_2@C core-shell nanowires were constructed on the titanium foam.
- 3D hierarchical catalysts were obtained by growing Pt nanowires on the TiO_2@C.
- Pt/TiO_2@C exhibits much better methanol oxidation properties than commercial Pt/C.

ARTICLE INFO

Article history:
Received 17 June 2019
Received in revised form
24 August 2020
Accepted 7 September 2020
Available online 26 September 2020

Keywords:
Pt nanowires
Titanium oxide
Hierarchical

ABSTRACT

Three-dimensional (3D) hierarchical Pt/TiO_2@C core-shell nanowire networks with high surface area have been constructed via wet chemical approaches. The 3D TiO_2 nanowire framework was *in situ* synthesized within a porous titanium foam by hydrothermal method followed by carbon coating and self-assembled growth of ultrathin Pt nanowires. Structural characterization indicates that single crystalline ultrathin Pt nanowires of 3–5 nm in diameter were vertically distributed on the anatase TiO_2 nanowires covered with a 2–4 nm thin carbon layer. The 3D hierarchical Pt/TiO_2@C nanostructure demonstrates evidently higher catalytic activities towards methanol oxidation than the commercial Pt/C catalyst. The catalytic current density of the hierarchical catalyst is 1.6 times as high as that of the commercial Pt/C, and the oxidation onset potential (0.35 V vs. Ag/AgCl) is more negative than the commercial one (0.46 V vs. Ag/AgCl). Synergistic effect between the ultrathin Pt nanowires and the TiO_2@C core-shell nanostructure accounts for the enhanced

* *Corresponding author*. School of Materials Science and Engineering, Hefei University of Technology, Hefei, 230009, PR China.
E-mail addresses: zhangyong.mse@hfut.edu.cn, zy_mse@126.com (Y. Zhang).
https://doi.org/10.1016/j.ijhydene.2020.09.052

Carbon coating
Methanol oxidation

catalytic properties, which can be determined by X-ray photoelectron spectroscopy (XPS) investigation. The obtained hierarchical Pt/TiO_2@C nanowire networks promise great potential in producing anode catalysts for direct methanol fuel cells applications.

Introduction

Fuel cells can convert chemical energy directly into electrical energy with high efficiency and almost zero-emission, which promises great potential for developing sustainable energy to alleviate the shortage of fossil fuels as well as environmental pollution [1–5]. Among various fuel cells, direct methanol fuel cells (DMFCs) have the advantages of high energy densities, facile fuel storage and transportation, good safety and low operating temperatures [6–11]. In the DMFCs, platinum-based catalysts are the most prevalent and efficient noble catalysts [12–14]. However, high cost of platinum has limited its large-scale application [15–18], while it remains greatly challengeable to make Pt replaceable. Recently, structural manipulation of Pt in nanoscale has attracted great attention, in which Pt nanowires exhibit enhanced electrocatalytic activity and more stable electrochemical properties [19–21] due to their ordered one-dimensional structure that more conducive to the mass transfer of electrode reactions [22].

On the other hand, commercial carbon black substrates for supporting Pt catalyst suffer from corrosion effect that leads to aggregation and loss of Pt especially at the high potential area. In addition, inert surface characteristics of the carbon black also restrict performance of the fuel cells [23–27]. During the exploration of new catalyst supports, titanium oxide is considered as one of the most promising catalyst substrates in terms of high corrosion resistance and electrochemical stability, cost effectiveness [27–30] as well as strong synergistic effect with platinum in enhancing the catalytic properties [31]. Nevertheless, low electrical conductivity of titanium oxide restricts its potential as an efficient catalyst support [32]. And as a new metal material, titanium foam has the dual function of foam structure and titanium, and has high strength, shock absorption, and damping properties. Using it as a substrate can not only maintain the characteristics of the porous structure, but also improve its surface activity and electrical conductivity [33]. Therefore, it is expected to design novel catalyst systems with high surface area, superior electrical conductivity and high durability [33,34], which can greatly utilize low loading Pt with competitive catalytic performance [35–37].

In this article, three dimensional hierarchical Pt/TiO_2@C nanowire networks have been constructed. It can be intuitively understood the preparation process of Pt/TiO_2@C from the schematic diagram as shown in Fig. 1. Firstly, three dimensional titanium oxide nanowire networks were *in situ* synthesized within a porous titanium metal foam which provides high specific surface area for active sites, mass transport and side reaction product removal. Secondly, the TiO_2@C core-shell nanowires were formed by coating a thin carbon layer to obtain high electrical conductivity [38–40]. Thirdly, ultrathin Pt nanowires were obtained on the surface of the TiO_2@C core-shell nanowires by a self-assembly method. In this case, the titanium foam can be regarded as both a substrate and a current collector owing to its excellent electrical conductivity. Finally, hierarchical Pt/TiO_2@C nanowire networks with 3D architecture were successfully constructed.

Experimental

Chemicals and materials

Titanium foam was purchased from Kunshan Kunping Lake Electronic Technology Co., Ltd., with a purity of 99.9%. Sodium hydroxide (NaOH), chloroplatinic acid hexahydrate ($H_2PtCl_6 \cdot 6H_2O$, AR, Pt 37.5%), hydrochloric acid, formic acid and glucose were acquired from Sinopharm Chemical Reagent Company. All chemicals were used without any further purification. High-purity milli-Q water was used in all experiments.

Synthesis of titanium oxide

Titanium oxide nanowires were *in situ* prepared by hydrothermal method followed by annealing treatment [41]. The experiment was divided into three steps. The preparation process needs to be very careful because we must strictly control the hydrothermal temperature, air flow and time during carbonization, and formic acid reduction time. During the experiment, 1 cm × 1 cm titanium foam was ultrasonicated in acetone, ethanol and deionized water, respectively, for 15 min. Then, titanium foam and NaOH solution (1 mol L^{-1}) were sealed into a Teflon-lined stainless-steel autoclave and heated at 220 °C for 24 h. After cooling to room temperature, the titanium foam was rinsed with deionized water and soaked in a 5% dilute hydrochloric acid solution for 15 min. And then washed several times with deionized water to pH ≈ 7. Finally, the sample was annealed at 600 °C in air to form titanium oxide.

Synthesis of carbon-coated titanium oxide

Titanium oxide was immersed in a 1 mol L^{-1} glucose solution for 1 h and then dried. Afterwards, the samples were incubated at 800 °C for 2 h in Ar atmosphere [42].

Preparation of Pt/TiO_2@C

The 600 μL 20 mmol L^{-1} solutions of H_2PtCl_6 was reduced by formic acid (HCOOH), then the titanium foam was put in the

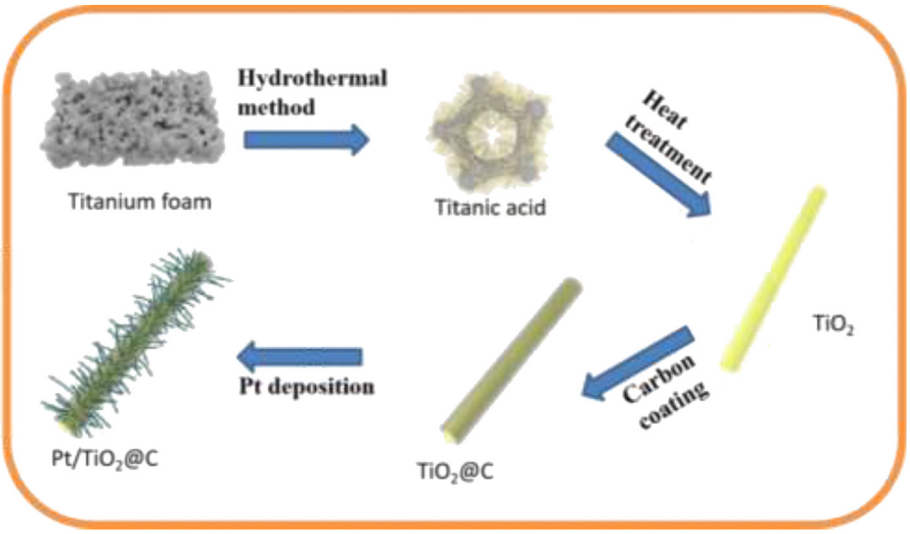

Fig. 1 – Schematic diagram of the Pt/TiO_2@C catalyst preparation process.

formic acid solution for 48 h to synthesize Pt nanowires on the TiO_2@C nanowires at 20 °C [36].

Characterization of physical properties and electrochemical measurements

Morphology, composition, structure and electrochemical properties of the anode material were characterized by SU8020 scanning electron mi-croscope (SEM), operated at 5 kV, JEM-2010F high-resolution transmission electron mi-croscope (HRTEM), operated at 200 kV, Rigaku D/MAX2500V X-ray diffractometer, Thermo ESCALAB 250 X-ray photoeletron spectrometer (XPS). The electrochemical measurements were carried out on an electrochemical workstation (CHI760E, Shanghai CH Instrument Company, China) which has a three-electrode experimental setup at ambient temperature. Platinum sheet electrode, Ag/AgCl electrode, Pt/TiO_2@C were used as counter electrode, reference electrode, working electrode, respectively. The working electrode was 1 cm × 1 cm titanium foam, to ensure that the contact area between the working electrode and the electrolyte is 0.25 cm^2. Sweep speed during electrochemical test was 50 mV/s.

Results and discussion

Fig. 2 (a) shows FESEM image of the TiO_2 NWs grown within the Ti foam, suggesting uniform, high density and three-dimensional architecture of the nanowires. Close-up observation of the carbon coated TiO_2 NWs as shown in Fig. 2 (b) suggests no obvious morphology difference to the pristine TiO_2 nanowires. The TiO_2 NWs have the diameter in a typical range between of 50–100 nm and length of about 1.5 μm. Fig. 2 (c) displays a typical HRTEM image of a single TiO_2@C core-shell nanowire, in which the surface of TiO_2 NW is covered with a uniform amorphous carbon layer with the measured thickness of around 3.2 nm. The lattice fringes in the HRTEM image of the nanowire core is determined to be 0.35 nm, which is designated to (101) crystal plane of anatase TiO_2 phase, as show in Fig. 2 (c). Fig. 2 (d) shows a bright field TEM

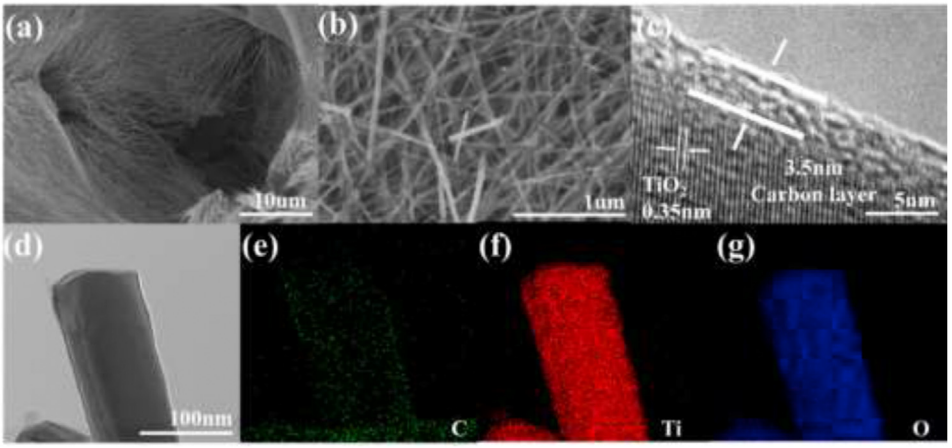

Fig. 2 – (a) SEM image with magnification of 5 k; (b) SEM image with magnification of 45 k; (c) HRTEM image of the TiO_2@C; (d), (e), (f) and (g) Elemental mapping of TiO_2@C.

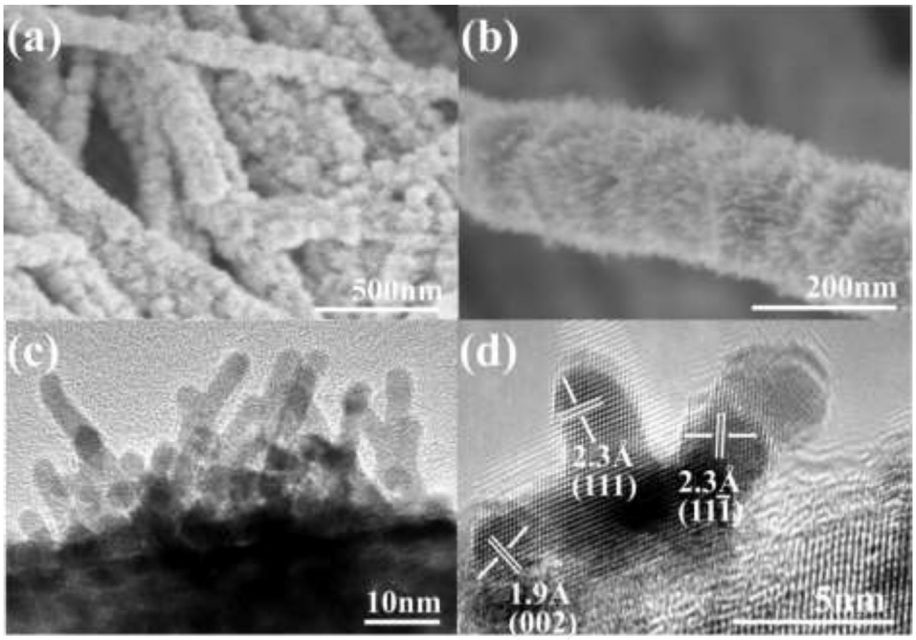

Fig. 3 – (a) SEM image of the Pt/TiO_2@C nanowires with magnification of 70K; (b) SEM image of the Pt/TiO_2@C nanowire with magnification of 200 K; (c) TEM micrograph of Pt nanowires grown on the surface of TiO_2@C nanowires; (d) HRTEM micrograph of several Pt nanowires grown onTiO_2@C.

image of a single TiO_2@C core-shell nanowire, and Fig. 2 (e, f, g) demonstrate the elemental mapping of Ti, O, C of the nanowire, respectively. Dense distribution of the Ti and O elements evidence the TiO_2 nanocore, while the low concentration but larger diameter of the carbon element profile suggests the carbon shell.

Fig. 3 (a) shows low magnification FESEM image of the Pt/TiO_2@C nanowire networks, demonstrating the uniform growth of the three dimensional hierarchical nanostructures with high density. The high magnification FESEM image as shown in Fig. 3 (b) show that the ultrathin Pt nanowires are uniformly distributed on the TiO_2@CNWs. The Pt NWs/TiO_2@C NWs were characterized by TEM. Fig. 3 (c) showing that Pt nanowires have the diameter of 3–5 nm and length of 5–10 nm. Fig. 3 (d) shows lattice stripes image of the Pt nanowires. The interplanar spacing of 2.3 Å corresponds to the (111) plane, and that of 1.9Å can be indexed to the (002) plane.

Phase structure of the Pt/TiO_2@C and TiO_2@C samples was characterized by XRD patterns as shown in Fig. 4 (a). The main characteristic diffraction peaks (2 θ = 40.0°, 46.5°, 67.8°) prove the presence of crystalline platinum loaded on the TiO_2@C. The standard reflection peaks of TiO_2@C reveal the existence of anatase TiO_2 and a small amount of rutile TiO_2. No diffraction peaks of carbon is present in the XRD pattern due to thin thickness and low crystallinity of the carbon, but the carbon layer can be confirmed by Raman spectroscopy. There are two broad Raman characteristic peaks as shown in Fig. 4 (b), which are D-bands at around 1360 cm^{-1} and G-bands at around 1587 cm^{-1}. The I_D/I_G is 0.91, 0.99 and 1.02, when the

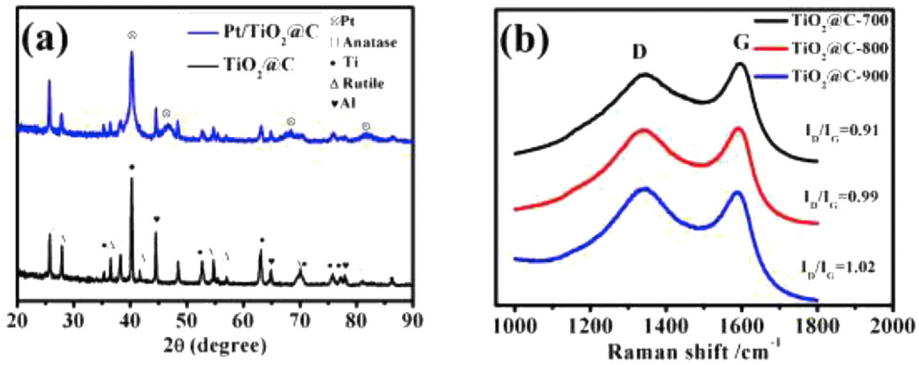

Fig. 4 – (a) XRD image of the Pt/TiO_2@C and TiO_2@C sample; (b) Raman image of TiO_2@C sample.

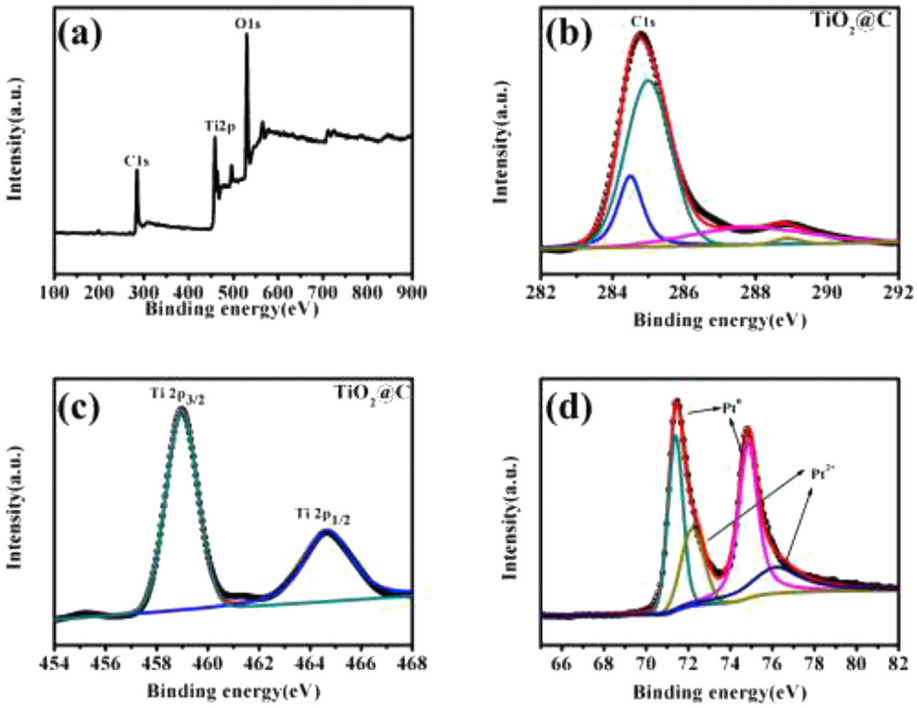

Fig. 5 – The results of XPS survey (a) XPS full spectrum of TiO_2@C; (b) C 1s of TiO_2@C; (c) Ti 2p of TiO_2@C; (d) Pt 4f of Pt/TiO_2@C.

carbonization temperatures is 700 °C, 800 °C and 900 °C, respectively. The stronger the intensity of G peak, the greater the number of graphite-like crystallites in the carbide and the number of carbon atoms at the edge of the graphite-like crystallites, and the carbonization of the product is increased [43]. This means that the conductivity of the substrate can be improved. At a high temperature of 900 °C, the titanium foam becomes brittle and the titanium oxide easily peels off from the titanium foam. We coated the carbon at 800 °C to ensure the stability of the catalyst substrate and excellent conductivity.

The chemical environment of samples was analyzed by X-ray photoelectron spectroscopy. Fig. 5 (a) displays the survey spectrum of the Pt/TiO_2@C hybrids, showing the existence of Ti, O, Pt and C elements. Fig. 5 (b) shows the spectrum collected from the C1s core level, the characteristic peaks at binding energies of 284.5, 285, 287.8 and 288.9 eV correspond to the aliphatic/aromatic carbon groups, amorphous carbon, carbonyl groups, carboxylic groups, esters or lactones [38,44,45]. Two broad peaks in Fig. 5 (c) reveal high resolution Ti 2p spectrum, in which the binding energy peaks centered at 464.7 and 459 eV correspond to the characteristic Ti $2p_{1/2}$ and Ti $2p_{3/2}$ peaks of Ti^{4+} [46], suggesting that the signals of the titanium oxide is not screened by the thin carbon layer. Fig. 5 (d) shows that the two peaks with the binding energy of 71.4 eV and 74.8 eV correspond to the metal titanium platinum in the Pt/TiO_2@C catalyst [47]. Two other weak peaks of Pt^{2+} may be due to the slight surface oxidation of the dense Pt nanowires. The surface of Pt^0 would provide more suitable sites for methanol electro-oxidation. It is essential for high surface activity with respect to methanol electro-oxidation [6].

Electrochemical behaviors of the Pt/TiO_2@C and Pt/C samples were evaluated by cyclic voltammograms (CVs) in 0.5 M H_2SO_4 solution as shown in Fig. 6 (a). The electrochemically active surface area (ECSA, m^2/g_{Pt}) of the Pt/C and Pt/TiO_2@C can be estimated according to the following equation [48]. It is calculated that the ECSA of the commercial Pt/C is 43 m^2/g, while the ECSA is 24.7 m^2/g for the Pt NWs on the

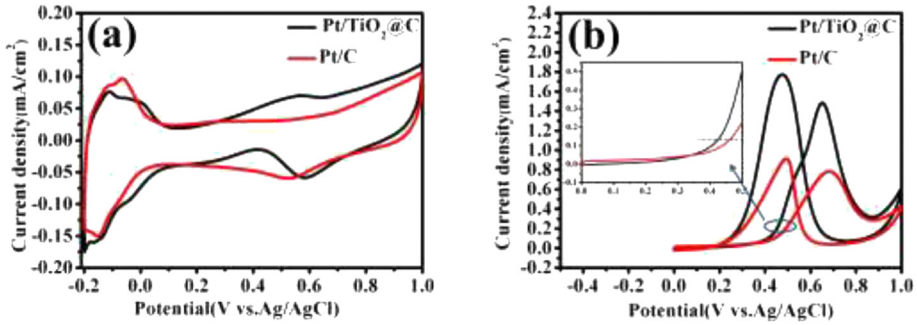

Fig. 6 – (a) Cyclic Voltammograms (CVs) of the Pt/C and Pt/TiO_2@C in 0.5 M H_2SO_4 solution; (b) in 0.5 M H_2SO_4 and 1 M CH_3OH, sweep speed is 50 mV/s.

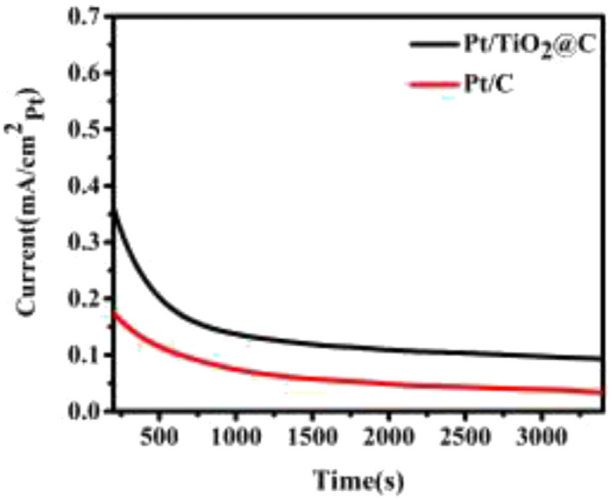

Fig. 7 – Amperometric i-t curves of Pt/C and Pt/TiO_2@C in 0.5 mol L^{-1} H_2SO_4 and 1 mol L^{-1} CH_3OH solution.

TiO_2@C nanowires. The actual content of Pt was determined by an inductively coupled plasma mass spectrometer (ICP) model Agilent 7500cx, which was about 10% [36].

$$ECSA = \frac{S_H/V}{0.21(mC/cm^2)\cdot M_{Pt}}$$

The electrocatalytic performance of the Pt/TiO_2@C toward methanol oxidation was evaluated by cyclic voltammetry in a 0.5 M H_2SO_4 aqueous solution containing 1 M CH_3OH at room temperature. As shown in Fig. 6 (b), it is observed that the specific peak current density (i.e, the forward anodic peak) of the Pt/TiO_2@C catalysts is 1.2 mA/cm^2_{Pt}, almost twice as high as that of the commercial Pt/C (0.76 mA/cm^2_{Pt}) though the electrochemically active surface area of the Pt/TiO_2@C is even much lower. In addition, the oxidation onset potential of Pt/TiO_2@C is 0.35 V, more negative than that of the commercial Pt/C of 0.46 V, suggesting higher catalytic activity of the hierarchical Pt/TiO_2@C catalyst.

The stability of the catalsyt was tested and the test potential at the i-t curve was 0.6 V which can be seen from Fig. 7, suggesting that the catalyst Pt/TiO_2@C had maintained high current density, and in the 3500s test, the current density retention rate of the catalyst Pt/TiO_2@C was 20%. And the methanol oxidation current density retention rate of Pt/C was 10%, revealing better electrochemical stability of the Pt/TiO_2@C catalyst. On the one hand, the anisotropic characteristics of small Pt nanowires are conducive to electron transport. On the other, compared with other works [37], Pt nanowires are thinner and more uniform, and have a larger specific surface area, which also enhances the electrocatalytic performance.

Conclusion

3D hierarchical Pt/TiO_2@C nanowire networks have been obtained using wet chemical methods. The Pt/TiO_2@C exhibits an enhanced electrocatalytic activity toward methanol oxidation compared to commerical Pt/C catalysts, in which the Pt/TiO_2@C catalysts possess much higher catalytic current density and more negative oxidation onset potential. The enhanced catalytic performance of the hierarchical nanowires can be ascribed to the synergistic effect between the ultrathin Pt nanowires and the TiO_2@C core shell structure as well as improved electrical conductivity contributed by the thin carbon shell. The present work proposes that the Pt/TiO_2@C nanowire networks are expected to be a promising anode catalysts in DMFC applications.

Declaration of competing interest

The authors declare that they have no known competing financial interests or personal relationships that could have appeared to influence the work reported in this paper.

Acknowledgements

This project is financially supported by the National Natural Science Foundation of China (Grant no.51772072), the Foundation for Tianchang Intelligent Equipment and Instruments Research Institute (Grant No. JZ2017AHDS1147), the Natural Science Foundation of Anhui Province (1708085ME100) and the 111 Project (B18018).

REFERENCES

[1] Cheng N, Shao Y, Liu J, Sun X. Electrocatalysts by atomic layer deposition for fuel cell applications. Nanomater Energy 2016;29:220–42. https://doi.org/10.1016/j.nanoen.2016.01.016.
[2] Song Z, Wang B, Cheng N, Yang L, Banham D, Li R, et al. Atomic layer deposited tantalum oxide to anchor Pt/C for a highly stable catalyst in PEMFCs. J Mater Chem 2017;5:9760–7. https://doi.org/10.1039/C7TA01926B.
[3] Li Y, Gao W, Ci L, Wang C, Ajayan PM. Catalytic performance of Pt nanoparticles on reduced graphene oxide for methanol electro-oxidation. Carbon 2010;48:1124–30. https://doi.org/10.1016/j.carbon.2009.11.034.
[4] Isaifan RJ, Couillard M, Baranova EA. Low temperature-high selectivity carbon monoxide methanation over yttria-stabilized zirconia-supported Pt nanoparticles. Int J Hydrogen Energy 2017;42:13754–62. https://doi.org/10.1016/j.ijhydene.2017.01.049.
[5] He D, Tang H, Kou Z, Pan M, Sun X, Zhang J, et al. Engineered graphene materials: synthesis and applications for polymer electrolyte membrane fuel cells. Adv Mater 2017;29:1601741. https://doi.org/10.1002/adma.201601741.
[6] Park KW, Choi JH, Lee SA, Pak C, Chang H, Sung Y-E. PtRuRhNi nanoparticle electrocatalyst for methanol electrooxidation in direct methanol fuel cell. J Catal 2004;224:236–42. https://doi.org/10.1016/j.jcat.2004.02.010.
[7] Uchida H, Mizuno Y, Watanabe M. Suppression of methanol crossover and distribution of ohmic resistance in Pt-dispersed PEMs under DMFC operation. J Electrochem Soc 2002;149:A682. https://doi.org/10.1149/1.1471539.
[8] Aricò AS, Srinivasan S, Antonucci V. DMFCs: from fundamental aspects to technology development. Fuel Cell 2001;1:133–61. https://doi.org/10.1002/1615-6854(200107)1:2<133::AID-FUCE133>3.0.CO;2-5.

[9] Lufrano F, Baglio V, Staiti P, Antonucci V, Arico AS. Performance analysis of polymer electrolyte membranes for direct methanol fuel cells. J Power Sources 2013;243:519–34. https://doi.org/10.1016/j.jpowsour.2013.05.180.

[10] Verjulio RW, Santander J, Sabaté N, Esquivel JP, Torres-Herrero N, Habrioux A, et al. Fabrication and evaluation of a passive alkaline membrane micro direct methanol fuel cell. Int J Hydrogen Energy 2014;39:5406–13. https://doi.org/10.1016/j.ijhydene.2013.12.014.

[11] Wang YJ, Qiao J, Baker R, Zhang J. Alkaline polymer electrolyte membranes for fuel cell applications. Chem Soc Rev 2013;42:5768–87. https://doi.org/10.1039/C3CS60053J.

[12] Chen J, Minett AI, Liu Y, Lynam C, Sherrell P, Wang C, et al. Cover picture: direct growth of flexible carbon nanotube electrodes. Adv Mater 2008;3. https://doi.org/10.1002/adma.200890007. Advanced Materials. 2008;20.

[13] Dicks AL. The role of carbon in fuel cells. J Power Sources 2006;156:128–41. https://doi.org/10.1016/j.jpowsour.2006.02.054.

[14] Lomocso TL, Baranova EA. Electrochemical oxidation of ammonia on carbon-supported bi-metallic PtM (M=Ir, Pd, SnO_x) nanoparticles. Electrochim Acta 2011;56:8551–8. https://doi.org/10.1016/j.electacta.2011.07.041.

[15] Zhao Y, Fan L, Zhong H, Li Y, Yang S. Platinum nanoparticle clusters immobilized on multiwalled carbon nanotubes: electrodeposition and enhanced electrocatalytic activity for methanol oxidation. Adv Funct Mater 2007;17:1537–41. https://doi.org/10.1002/adfm.200600416.

[16] Borup R, al e, et al. Scientific aspects of polymer electrolyte fuel cell durability and degradation. ChemInform 2007;38. https://doi.org/10.1002/chin.200750270.

[17] Cheng N, Stambula S, Wang D, Banis MN, Liu J, Riese A, et al. Platinum single-atom and cluster catalysis of the hydrogen evolution reaction. Nat Commun 2016;7:13638. https://doi.org/10.1038/ncomms13638.

[18] Li J, Song Y, Zhang G, Liu H, Wang Y, Sun S, et al. Pyrolysis of self-assembled iron porphyrin on carbon black as core/shell structured electrocatalysts for highly efficient oxygen reduction in both alkaline and acidic medium. Adv Funct Mater 2017;27:1604356. https://doi.org/10.1002/adfm.201604356.

[19] Sakamoto Y, Fukuoka A, Higuchi T, Shimomura N, Inagaki S, Ichikawa M. Synthesis of platinum nanowires in organic-inorganic mesoporous silica templates by photoreduction: formation mechanism and isolation. J Phys Chem B 2004;108:853–8. https://doi.org/10.1021/jp036617v.

[20] Han YJ, Kim JM, Stucky GD. Preparation of noble metal nanowires using hexagonal mesoporous silica SBA-15. Chem Mater 2000;12:2068–9. https://doi.org/10.1021/cm0010553.

[21] Shen Z, Yamada M, Miyake M. Preparation of single-crystalline platinum nanowires with small diameters under mild conditions. Chem Commun 2007:245–7. https://doi.org/10.1039/B613895K.

[22] Yan Z, Li B, Yang D, Ma J. Pt nanowire electrocatalysts for proton exchange membrane fuel cells. Chin J Catal 2013;34:1471–81. https://doi.org/10.1016/S1872-2067(12)60629-9.

[23] Avasarala B, Haldar P. Electrochemical oxidation behavior of titanium nitride based electrocatalysts under PEM fuel cell conditions. Electrochim Acta 2010;55:9024–34. https://doi.org/10.1016/j.electacta.2010.08.035.

[24] Avasarala B, Moore R, Haldar P. Surface oxidation of carbon supports due to potential cycling under PEM fuel cell conditions. Electrochim Acta 2010;55:4765–71. https://doi.org/10.1016/j.electacta.2010.03.056.

[25] Shao Y, Yin G, Gao Y. Understanding and approaches for the durability issues of Pt-based catalysts for PEM fuel cell. J Power Sources 2007;171:558–66. https://doi.org/10.1016/j.jpowsour.2007.07.004.

[26] Abdullah M, Kamarudin SK, Shyuan LK. TiO_2 Nanotube-carbon (TNT-C) as support for Pt-based catalyst for high methanol oxidation reaction in direct methanol fuel cell. Nanoscale Research Letters 2016;11:553. https://doi.org/10.1186/s11671-016-1587-2.

[27] Jiang ZZ, Wang ZB, Chu YY, Gu DM, Yin GP. Ultrahigh stable carbon riveted Pt/TiO_2-C catalyst prepared by in situ carbonized glucose for proton exchange membrane fuel cell. Energy Environ Sci 2011;4:728–35. https://doi.org/10.1039/C0EE00475H.

[28] Prakash J, Sun S, Swart HC, Gupta RK. Noble metals-TiO_2 nanocomposites: from fundamental mechanisms to photocatalysis, surface enhanced Raman scattering and antibacterial applications. Applied Materials Today 2018;11:82–135. https://doi.org/10.1016/j.apmt.2018.02.002.

[29] Ge M, Cao C, Huang J, Li S, Chen Z, Zhang KQ, et al. A review of one-dimensional TiO_2 nanostructured materials for environmental and energy applications. J Mater Chem 2016;4:6772–801. https://doi.org/10.1039/C5TA09323F.

[30] Sharma S, Pollet BG. Support materials for PEMFC and DMFC electrocatalysts-A review. J Power Sources 2012;208:96–119. https://doi.org/10.1016/j.jpowsour.2012.02.011.

[31] Lv Q, Yin M, Zhao X, Li C, Liu C, Xing W. Promotion effect of TiO_2 on catalytic activity and stability of Pt catalyst for electrooxidation of methanol. J Power Sources 2012;218:93–9. https://doi.org/10.1016/j.jpowsour.2012.06.051.

[32] Lee JM, Han SB, Song YJ, Kim JY, Roh B, Hwang I, et al. Methanol electrooxidation of Pt catalyst on titanium nitride nanostructured support. Appl Catal Gen 2010;375:149–55. https://doi.org/10.1016/j.apcata.2009.12.037.

[33] Dunand DC. Processing of titanium foams. Adv Eng Mater 2004;6:369–76. https://doi.org/10.1002/adem.200405576.

[34] Avasarala B, Haldar P. On the stability of TiN-based electrocatalysts for fuel cell applications. Int J Hydrogen Energy 2011;36:3965–74. https://doi.org/10.1016/j.ijhydene.2010.12.107.

[35] Haldorai Y, ArreagaSalas D, Rak CS, Huh YS, Han YK, Voit W. Platinized titanium nitride/graphene ternary hybrids for direct methanol fuel cells and titanium nitride/graphene composites for high performance supercapacitors. Electrochim Acta 2016;220:465–74. https://doi.org/10.1016/j.electacta.2016.10.130.

[36] Sun S, Jaouen F, Dodelet JP. Controlled growth of Pt nanowires on carbon nanospheres and their enhanced performance as electrocatalysts in PEM fuel cells. Adv Mater 2008;20:3900–4. https://doi.org/10.1002/adma.200800491.

[37] Zheng L, Yang D, Chang R, Wang C, Zhang G, Sun S. Crack-tips enriched platinum-copper superlattice nanoflakes as highly efficient anode electrocatalysts for direct methanol fuel cells. Nanoscale 2017;9:8918–24. https://doi.org/10.1039/C7NR02570J.

[38] Sui XL, Wang ZB, Li CZ, Zhang JJ, Zhao L, Gu DM. Effect of core/shell structured TiO_2@C nanowire support on the Pt catalytic performance for methanol electrooxidation. Catal Sci Technol 2016;6:3767–75. https://doi.org/10.1039/C5CY02188J.

[39] Sui XL, Gu DM, Wang ZB, Liu J, Zhao L, Zhang LM. Three-dimensional TiO_2@C nano-network with high porosity as a highly efficient Pt-based catalyst support for methanol electrooxidation. RSC Adv 2016;6:79254–62. https://doi.org/10.1039/C6RA17542B.

[40] Xia T, Zhang W, Wang Z, Zhang Y, Song X, Murowchick J, et al. Amorphous carbon-coated TiO_2 nanocrystals for improved lithium-ion battery and photocatalytic performance. Nanomater Energy 2014;6:109–18. https://doi.org/10.1016/j.nanoen.2014.03.012.

[41] Liu E, Hu Y, Li H, Tang C, Hu X, Fan J, et al. Photoconversion of CO_2 to methanol over plasmonic Ag/TiO_2 nano-wire films enhanced by overlapped visible-light-harvesting nanostructures. Ceram Int 2015;41:1049–57. https://doi.org/10.1016/j.ceramint.2014.09.027.

[42] Devarapalli RR, Szunerits S, Coffinier Y, Shelke MV, Boukherroub R. Glucose-derived porous carbon-coated silicon nanowires as efficient electrodes for aqueous micro-supercapacitors. ACS Appl Mater Interfaces 2016;8:4298–302. https://doi.org/10.1021/acsami.5b11240.

[43] Meng W, Du X, Lin Z, Li W. Facile flame deposition of carbon coating onto Ni foam and the study of the derived carbon foam with high capacitive performance. Surf Coating Technol 2020;401:126246. https://doi.org/10.1016/j.surfcoat.2020.126246.

[44] Okpalugo TIT, Papakonstantinou P, Murphy H, McLaughlin J, Brown NMD. High resolution XPS characterization of chemical functionalised MWCNTs and SWCNTs. Carbon 2005;43:153–61. https://doi.org/10.1016/j.carbon.2004.08.033.

[45] Xia W, Wang Y, Bergsträßer R, Kundu S, Muhler M. Surface characterization of oxygen-functionalized multi-walled carbon nanotubes by high-resolution X-ray photoelectron spectroscopy and temperature-programmed desorption. Appl Surf Sci 2007;254:247–50. https://doi.org/10.1016/j.apsusc.2007.07.120.

[46] Zhang M, Shao C, Guo Z, Zhang Z, Mu J, Cao T, et al. Hierarchical nanostructures of copper(II) phthalocyanine on electrospun TiO_2 nanofibers: controllable solvothermal-fabrication and enhanced visible photocatalytic properties. ACS Appl Mater Interfaces 2011;3:369–77. https://doi.org/10.1021/am100989a.

[47] Batalović K, Bundaleski N, Radaković J, Abazović N, Mitrić M, Silva RA, et al. Modification of N-doped TiO_2 photocatalysts using noble metals (Pt, Pd)-a combined XPS and DFT study. Phys Chem Chem Phys 2017;19:7062–71. https://doi.org/10.1039/C7CP00188F.

[48] Xu H, Ding LX, Feng JX, Li GR. Pt/$Ni(OH)_2$-NiOOH/Pd multi-walled hollow nanorod arrays as superior electrocatalysts for formic acid electrooxidation. Chem Sci 2015;6:6991–8. https://doi.org/10.1039/C5SC02544C.